



# Discovery of dapivirine, a nonnucleoside HIV-1 reverse transcriptase inhibitor, as a broad-spectrum antiviral against both influenza A and B viruses



Yanmei Hu <sup>a,1</sup>, Jiantao Zhang <sup>a,1</sup>, Rami Ghassan Musharrafieh <sup>b</sup>, Chunlong Ma <sup>c</sup>,  
Raymond Hau <sup>b</sup>, Jun Wang <sup>a,c,\*</sup>

<sup>a</sup> Department of Pharmacology and Toxicology, College of Pharmacy, University of Arizona, Tucson, AZ 85721, United States

<sup>b</sup> Department of Chemistry and Biochemistry, University of Arizona, Tucson, AZ 85721, United States

<sup>c</sup> BIO5 Institute, University of Arizona, Tucson, AZ 85721, United States

## ARTICLE INFO

### Article history:

Received 9 June 2017

Received in revised form

26 July 2017

Accepted 27 July 2017

Available online 2 August 2017

### Keywords:

Influenza virus

Dapivirine

Broad-spectrum antiviral

Drug resistance

Dual antiviral

## ABSTRACT

The emergence of multidrug-resistant influenza viruses poses a persistent threat to public health. The current prophylaxis and therapeutic interventions for influenza virus infection have limited efficacy due to the continuous antigenic drift and antigenic shift of influenza viruses. As part of our ongoing effort to develop the next generation of influenza antivirals with broad-spectrum antiviral activity and a high genetic barrier to drug resistance, in this study we report the discovery of dapivirine, an FDA-approved HIV nonnucleoside reverse transcriptase inhibitor, as a broad-spectrum antiviral against multiple strains of influenza A and B viruses with low micromolar efficacy. Mechanistic studies revealed that dapivirine inhibits the nuclear entry of viral ribonucleoproteins at the early stage of viral replication. As a result, viral RNA and protein synthesis were inhibited. Furthermore, dapivirine has a high *in vitro* genetic barrier to drug resistance, and its antiviral activity is synergistic with oseltamivir carboxylate. In summary, the *in vitro* antiviral results of dapivirine suggest it is a promising candidate for the development of the next generation of dual influenza and HIV antivirals.

© 2017 Elsevier B.V. All rights reserved.

## 1. Introduction

The influenza viruses are negative-sense, single-stranded, segmented RNA viruses that belong to the family of *Orthomyxoviruses* (Palese and Shaw, 2007). There are three types of influenza viruses: A, B, and C. Influenza A virus is the most virulent human pathogen among the three types and leads to the most severe disease outcomes. Influenza A viruses are the causative agents for both seasonal influenza and pandemic influenza. It is estimated that 3–5 million infections and 250,000–500,000 deaths are associated with seasonal influenza virus infection worldwide (Thompson et al., 2010). In the event of an influenza pandemic, the impact is usually several orders of magnitude higher. For example, the 1918 Spanish H1N1 influenza claimed 40 million lives (Johnson

and Mueller, 2002), and the latest 2009 swine influenza pandemic led to approximately 284,000 deaths (Dawood et al., 2012). Besides influenza A viruses, influenza B viruses are also substantial human pathogens. Infection with influenza B viruses can be as severe as influenza A viruses, especially in children and immunocompromised patients (Koutsakos et al., 2016). Influenza A and B viruses co-circulate in each influenza season, and as a result, both the trivalent and quadrivalent influenza vaccines contain the viral components from influenza B viruses. In contrast, the influenza C virus, which infects humans, dogs, and pigs, is less common than influenza A or B and usually only causes mild disease in children (Matsuzaki et al., 2006).

There are two general strategies to combat influenza epidemics and pandemics: vaccines and small-molecule antiviral drugs (Loregian et al., 2014). Influenza vaccines are the first line of defense to prevent influenza virus infection, with an overall 60% effectiveness (Osterholm et al., 2012). For this reason, influenza vaccines are recommended for anyone aged six months or older with a few exceptions (Grohskopf et al., 2015). Although influenza vaccines are

\* Corresponding author. Room 423, 1657 E. Helen St., BIO5 Institute, Tucson, AZ 85721, United States.

E-mail address: [junwang@pharmacy.arizona.edu](mailto:junwang@pharmacy.arizona.edu) (J. Wang).

<sup>1</sup> Y.H. and J. Z. contributed equally to this work.

suitable for immune-competent persons, they have limited efficacy in immune-compromised patients (Osterholm et al., 2012). Moreover, there is usually a six-month delay between viral identification and vaccine production (Lambert and Fauci, 2010; Wong and Webby, 2013). Therefore, antiviral drugs are highly desired in combating the threat of influenza, especially at the early phase of influenza pandemic when influenza vaccines are not available. As a segmented RNA virus, influenza virus undergoes both antigenic shift and antigenic drift during viral replication. As a result, influenza viruses exist in quasispecies and have a diverse genetic background (Lauring and Andino, 2010). Although the genetic diversity is beneficial to the virus's survival, this poses a grand challenge in devising antiviral drugs. Currently, there are two classes of FDA-approved antiviral drugs for the prophylaxis and treatment of influenza infection: the M2 ion channel blockers amantadine and rimantadine (Wang et al., 2011, 2015) and the neuraminidase (NA) inhibitors oseltamivir, zanamivir, and peramivir (Loregian et al., 2014). At present, more than 95% of currently circulating influenza A virus strains are resistant to amantadine and rimantadine, so they are no longer recommended (Wang et al., 2015). The majority of currently circulating influenza viruses remain sensitive to oseltamivir; however, the number of reports of oseltamivir-resistant influenza strains keeps increasing (Bloom et al., 2010; Hay and Hayden, 2013; Samson et al., 2013). The 2007–2008 seasonal H1N1 influenza virus in North America, which carries the H275Y mutation in the NA gene, was completely resistant to oseltamivir (Hurt, 2014). Collectively, the emergence of oseltamivir-resistant influenza viruses is a timely reminder of the urgent need for the next generation of antiviral drugs with a novel mechanism of action.

Drug repurposing, also known as drug repositioning or drug rescue, emerged primarily in the early 1990s as a viable alternative to the conventional *de novo* drug discovery and development approach (Novac, 2013). The terminology of drug repurposing refers to “the process of identifying new indications for existing drugs, abandoned or shelved compounds and candidates under development”. This approach yielded several classic drugs. One is sildenafil, which was originally discovered as a treatment for various cardiovascular disorders in 1989 and now is sold with the brand name Viagra to treat erectile dysfunction (Fink et al., 2002). Another is azidothymidine, which originally failed as a chemotherapy anticancer drug due to the lack of efficacy but emerged in the 1980s as a therapy for HIV (D'Andrea et al., 2008). Compared to traditional drug discovery and development, drug repositioning has significant advantages, such as minimal risk of failure since the toxicity, tolerance, and pharmacokinetic properties of repositioned drugs are already known. Therefore the cost and time needed to bring a drug to market are significantly reduced (Ashburn and Thor, 2004).

In the present work, we report the repurposing of dapivirine (Fig. 1A), an HIV nonnucleoside reverse transcriptase inhibitor (NNRTI), as a promising anti-influenza agent. Dapivirine (TMC120) was originally developed as an HIV NNRTI and formulated as an intravaginal ring to prevent the transmission of HIV (Nel et al., 2016) (Baeten et al., 2016). Two Phase 3 clinical trials of intravaginal dapivirine rings for HIV prevention were completed in 2015, and the results showed 27% and 31% reduction in HIV-1 acquisition, respectively (Nel et al., 2016). However, the antiviral activity of dapivirine in inhibiting influenza viruses has not been reported before. In this study, we discovered that dapivirine has broad-spectrum antiviral activity against both influenza A and B viruses. Dapivirine also has a high *in vitro* genetic barrier to drug resistance, and no resistant virus emerged under drug selection pressure. Mechanistic studies revealed that dapivirine inhibits the early stage of viral replication by restricting the nuclear entry of the

viral ribonucleoprotein (vRNP) complex. Due to its novel mechanism of action, dapivirine was also found to have a synergistic antiviral effect when combined with oseltamivir carboxylate.

Repurposing a HIV drug such as dapivirine as a broad-spectrum influenza antiviral is significant because HIV-infected patients are classified as high-risk group of serious influenza-related complications (<https://www.cdc.gov/flu/protect/hiv-flu.htm>). For example, an increased mortality rate was observed for patients at late and advanced HIV disease stages when infected with the 2009 pandemic H1N1 virus (Ormsby et al., 2011). Moreover, as immunocompromised patients require extended treatment with antiviral drugs in the event of influenza virus infection, emergence of drug-resistant influenza strains becomes a major concern (Trebien et al., 2017; van Kampen et al., 2013). Therefore, a dual HIV and influenza antiviral would be ideal to help protect HIV-infected patients from severe disease outcomes as well as circumvent drug resistance.

Collectively, the discovery of the broad-spectrum influenza antiviral activity of dapivirine provides a promising starting point for further development of dual HIV and influenza antivirals.

## 2. Materials and methods

### 2.1. Compounds, cell lines, viruses, and viral infection

Dapivirine (Cat #S2914), etravirine (Cat #S3080), and rilpivirine (Cat #S7303) were ordered from Selleckchem. Oseltamivir carboxylate was ordered from Santa Cruz Biotechnology (Cat # sc-212484). Madin-Darby Canine Kidney (MDCK) cells, adenocarcinomic human alveolar basal epithelial (A549) cells and human embryonic kidney (HEK293) cells were grown at 37 °C in 5% CO<sub>2</sub> atmosphere in DMEM media (high glucose, with L-glutamine) supplemented with 10% fetal bovine serum (FBS), 100 U/mL penicillin and 100 µg/mL streptomycin. MDCK cells overexpressing ST6Gal I (Shuji Hatakeyama et al., 2015) were obtained from Dr. Yoshihiro Kawaoka at the University of Wisconsin at Madison through a material transfer agreement and were maintained in the presence of 7.5 µg/mL puromycin, except when they were used for viral infection. Influenza A virus strains, A/California/07/2009 (H1N1) and A/Texas/04/2009 (H1N1), and influenza B virus strains, B/Brisbane/60/2008 (Victoria lineage) and B/Wisconsin/1/2010 (Yamagata lineage), were obtained from Dr. James Noah at the Southern Research Institute. Influenza A virus strains A/Denmark/524/2009 (H1N1) and A/Denmark/528/2009 (H1N1) were obtained from Dr. Elena Govorkova at St. Jude Children's Research Hospital. Influenza A virus strain A/Solomon Islands/3/2006 (H1N1) was obtained from Dr. Donald Smee at Utah State University. Influenza A virus strains A/Udorn/1972 (H3N2) and A/WSN/1933 (H1N1) were obtained from Dr. Robert Lamb at Northwestern University; and influenza A virus strains A/Switzerland/9715293/2013 (H3N2), A/Switzerland/9715293/2013 X-247 (H3N2), A/California/2/2014 (H3N2), A/Washington/29/2009 (H1N1), A/North Carolina/39/2009 (H1N1), A/Hong Kong/4801/2014 (H3N2) were obtained through the Influenza Reagent Resource, Influenza Division, WHO Collaborating Center for Surveillance, Epidemiology and Control of Influenza, Centers for Disease Control and Prevention, Atlanta, GA, USA. Viruses were amplified in MDCK cells in the presence of 2 mg/mL N-acetyl tryptase. Forty-eight hours p.i., the culture media were harvested and cell debris was removed by centrifugation at 3000 rpm for 30 min. Virus titers were determined by plaque assay using MDCK cells expressing ST6Gal I.

### 2.2. Plaque assay

A plaque assay was carried out as previously described (Li et al., 2016, 2017) except that MDCK cells expressing ST6Gal I were used

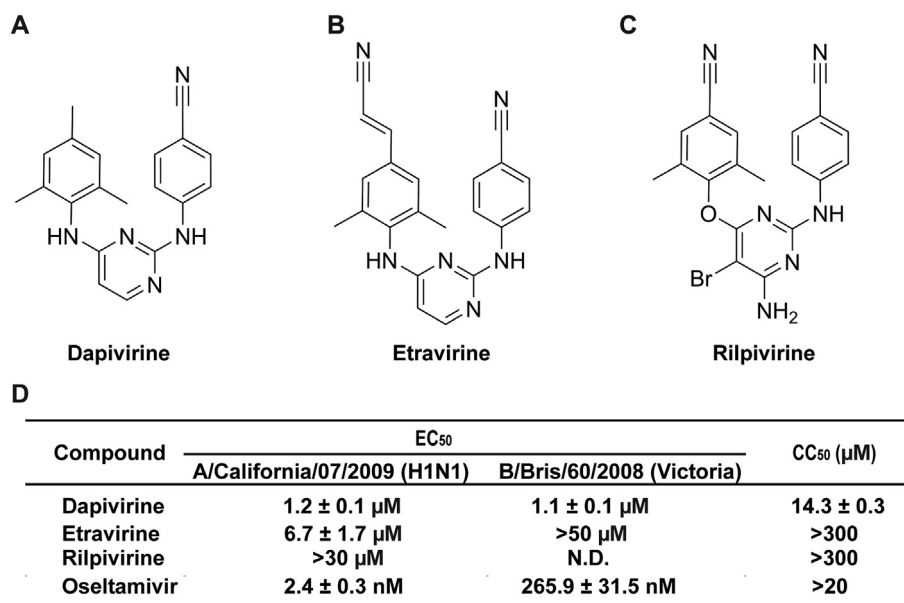


**Fig. 1. Chemical structures and antiviral activity of the three HIV NNTIs.** (A) Dapivirine; (B) Etravirine; (C) Rilpivirine; (D) EC<sub>50</sub> of the three NNTIs against A/California/07/2009 and B/Brisbane/60/2008 and CC<sub>50</sub> of the three NNTIs with a 48 h incubation time with MDCK cell line. The EC<sub>50</sub> and CC<sub>50</sub> values are the mean of two independent experiments ± standard deviation.

instead of regular MDCK cells.

### 2.3. Cytotoxicity assay and cytopathic effect (CPE) assay

Evaluation of the cytotoxicity of compounds and the efficacy of compounds against influenza virus-induced cytopathic effect were carried out using the neutral red uptake assay (Repetto et al., 2008). Briefly, 80,000 cells/mL MDCK or A549 cells in DMEM medium supplemented with 10% FBS and 100 U/mL penicillin-streptomycin were dispensed into 96-well cell culture plates at 100 μL/well. Twenty-four hours later, the growth medium was removed and washed with 100 μL PBS buffer. For the cytotoxicity assay, 200 μL fresh DMEM (no FBS) medium containing serial diluted compounds was added to each well. After incubating for 48 h at 37 °C with 5% CO<sub>2</sub> in a CO<sub>2</sub> incubator, the medium was removed and replaced with 100 μL DMEM medium containing 40 μg/mL neutral red for 4 h at 37 °C. The amount of neutral red taken up was determined by absorbance 540 nm using a Multiskan FC Microplate Photometer (Fisher Scientific). The CC<sub>50</sub> values were calculated from best-fit dose response curves with variable slope in Prism 5.

For the CPE assay, cells at 8000 cells/well density were infected with 100 μL of 100 PFU influenza virus A/WSN/1933 (H1N1) for 1 h at 37 °C. Unadsorbed virus was removed and the cells were treated with various doses of tested compounds (0, 0.3, 1, 3, 10, 30, 100 μM). The uninfected cells and oseltamivir carboxylate (Ma et al., 2016b) were included in each test as controls. The plates were incubated at 37 °C for 44–48 h, and neutral red was added when a significant cytopathic effect was observed in the wells without compound (virus only). The EC<sub>50</sub> values were calculated from best-fit dose response curves with variable slope in Prism 5.

### 2.4. Serial viral passage experiments

Two sets of serial viral passage experiments were performed. The first set was done with A/WSN/33 (H1N1) virus. MDCK cells were infected with the A/WSN/33 (H1N1) virus at MOI 0.001 for 1 h. Then the inoculum was removed and MDCK cells were incubated with 2 μM dapivirine in the first passage and the

concentration of dapivirine was gradually increased 2-fold in passages 2–3 and kept constant at 8 μM at passages 4 and onward. In each passage, the viruses were harvested when a significant cytopathic effect was observed, which usually takes 2–3 days after virus infection. The titers of harvested viruses were determined by plaque assay. The dapivirine sensitivity after passages 3, 6, 9, and 12 was determined via plaque assay as described previously (Hu et al., 2017). The second set of serial passage experiment was performed with the A/Switzerland/9715293/2013 (H3N2) virus. Experimental conditions were the same as for the first set except that the experiment was stopped at passage 6. Oseltamivir carboxylate was included as a control. The drug sensitivity of oseltamivir at passages 0, 3, and 6 was determined via plaque assay.

### 2.5. Time-of-addition experiment

A time-of-addition experiment was performed as previously described (Ma et al., 2016a). Briefly, MDCK cells were seeded at  $2 \times 10^5$  cells/6 cm dish. Oseltamivir carboxylate (1 μM) or dapivirine (3 μM) was added at different time points, as illustrated in Fig. 3. MDCK cells were infected with the A/WSN/33 (H1N1) virus at MOI 0.01 48 h after seeding. Viruses were harvested at 12 h after infection. The virus titers were determined by plaque assay. Oseltamivir carboxylate was included as a control.

### 2.6. Influenza virus mini-genome assay

A549 cells were seeded at  $3 \times 10^5$  cells per well in 12-well plates and incubated overnight at 37 °C, with 5% CO<sub>2</sub> in a CO<sub>2</sub> cell culture incubator. The cells were transfected with pCDNA constructs of the influenza A/WSN/33 (H1N1) virus PB1, PB2, and PA (100 ng each) and NP (200 ng), the RNA polymerase II-driven Renilla luciferase reporter pRL-SV40 (Promega) (250 ng), and the influenza virus-specific RNA polymerase I-driven firefly luciferase reporter (vRNA Luc) (250 ng). The transfection was performed with TransIT-293 (Mirus) in OptiMEM (Invitrogen). Two hours after transfection, the media was supplemented with 1 mL of compound to their final concentrations. Twenty-four hours after incubation, cells were

harvested, and firefly luciferase and Renilla luciferase expressions were determined using the Dual Luciferase Assay Kit (Promega).

### 2.7. RNA extraction and real-time PCR

Total RNA was extracted from the influenza A/WSN/33 (H1N1) infected cells using Trizol reagents (Thermo Fisher Scientific). After removing genomic DNA by RQ1 RNase-Free DNase (Promega), the first strand of cDNA was synthesized using 1.2 µg of total RNA and AMV Reverse Transcriptase (Promega). A vRNA-specific primer (5'-AGCAAAGCAGG-3'), cRNA-specific primer (5'-AGTAGAAACAAGG-3') or oligo (dT)<sub>18</sub> was used for detecting influenza vRNA, cRNA, or mRNA, respectively. Real-time PCR was performed on a StepOne-Plus Real-Time PCR System (Thermo Fisher Scientific) using FastStart Universal SYBR Green Master (Rox) and following influenza NP- or M1-specific primers: NP-F: 5'-AGGGTCAGTTGCT-CACAAGTCC-3'; NP-R: 5'-TTTGAAGCAGTCTGAAAGGGTCTA-3'; M1-F: 5'-ATGGGAACGGAGATCCAAATAA-3'; M1-R: 5'-TGCACCAGCA-GAATAACTGAGTG-3'. GAPDH was also amplified to serve as a control using human GAPDH-specific primers (HsGAPDH-F: 5'-ACACCCACTCCTCCACCTTG-3' and HsGAPDH-R: 5'-CAC-CACCCTGTGCTGTAGCC-3') or Canis GAPDH-specific primers (CIGAPDH-F: 5'-ACAGCAAATCCACGGCACA-3' and CIGAPDH-R: 5'-TACTCAGCACCAGCATCACCC-3'). The amplification conditions were 95 °C for 10 min, 40 cycles of 15 s at 95 °C, and 60 s at 60 °C. A melting curve analysis was performed to verify the specificity of each amplification. All experiments were repeated three times independently.

### 2.8. Western blotting

Total proteins were extracted using RAPI lysis buffer (50 mM Tris pH 8.0, 1% NP-40, 0.1% SDS, 150 mM NaCl, 0.5% sodium deoxycholate, 5 mM EDTA, 10 mM NaF, 10 mM NaPPi, 2 mM phenylmethylsulfonyl, and 1 mM PMSF). Equal amounts of extracted total proteins were separated by electrophoresis and transferred to a polyvinylidene difluoride (PVDF) membrane. Target protein was detected using the following antibodies and dilutions: rabbit anti-NP (GeneTex: GTX125989) at 1:5,000, rabbit anti-M1 (GeneTex: GTX125928) at 1:5,000, rabbit anti-NS1 (GeneTex: GTX125990) at 1:5,000, rabbit anti-HA (GeneTex: GTX127357) at 1:3,000, mouse anti-GAPDH antibody (EMD Millipore: MAB374) at 1:3000; detection used horseradish peroxidase-conjugated secondary antibodies at 1:3000 and Supersignal West Femto substrate (Thermo Scientific).

### 2.9. Immunostaining

Influenza A/WSN/33 (H1N1)-infected cells were fixed with 4% formaldehyde for 10 min followed by permeabilization with 0.2% Triton X-100 for another 10 min. After blocking with 10% bovine serum, cells were sequentially stained with mouse anti-NP antibody (Bio-Rad: MCA400), rabbit anti-M1 antibody (Genetex: GTX125928), and anti-mouse secondary antibody conjugated to Alexa-488 (Thermo Scientific). Nuclei were stained with 300 nM DAPI (Thermo Scientific) after secondary antibody incubation. Fluorescent images were acquired using a Leica SP5-II spectral confocal microscope in Cancer center of the University of Arizona.

### 2.10. Assessment of combination treatment of dapivirine with oseltamivir in vitro

The synergistic antiviral effects of dapivirine and oseltamivir carboxylate were evaluated in cell cultures as described previously (Huggins et al., 1984) using the CPE assay, as described in

“Cytotoxicity assay and cytopathic effect (CPE) assay” section above except that the compounds added were oseltamivir carboxylate or dapivirine, alone or in combination. Five combinations of dapivirine and oseltamivir, at the fixed EC<sub>50</sub> ratios of 10:1, 5:1, 1:1, 1:5, and 1:10, were included. In each combination, six 3-fold serial dilutions (equal to a 0.5 log<sub>10</sub> unit decrease) of the stock solution were tested to plot the dose inhibition curve, based on which the EC<sub>50</sub> values of individual dapivirine or oseltamivir were determined. Subsequently, the fractional inhibitory concentration index (FICI) was calculated using the following formula:  $FICI = [(EC_{50} \text{ of dapivirine in combination}) / (EC_{50} \text{ of dapivirine alone})] + [(EC_{50} \text{ of oseltamivir in combination}) / (EC_{50} \text{ of oseltamivir alone})]$ . FICI <0.5 was interpreted as a significant synergistic antiviral effect (Odds, 2003).

### 2.11. Data analysis

Data reported are the mean of two independent experiments ± standard deviation. In each independent experiments, all assays were performed in duplicates except the cytotoxicity assay, which was performed in eight replicates.

## 3. Results

### 3.1. Dapivirine has broad-spectrum antiviral activity against influenza A and B viruses

In a screening of an in-house library of compounds consisting of both known drugs and drug-like molecules, dapivirine (Fig. 1A) was identified as a potent antiviral against the A/California/07/2009 (H1N1) virus in the plaque assay (Hu et al., 2017). In the plaque assay, MDCK cells were infected with A/California/07/2009 (H1N1) at 100 PFU/well in the presence of increasing concentrations of dapivirine. After two days of incubation, cells were stained with crystal violet and the plaque area was quantified by Image J (49). It was found that dapivirine inhibited A/California/07/2009 (H1N1) replication in a dose-dependent manner with an EC<sub>50</sub> of 1.2 ± 0.1 µM (Fig. 1D). The cytotoxicity of dapivirine in MDCK cells was 14.3 ± 0.3 µM with 48 h incubation time (same as plaque assay); therefore, the observed antiviral effect was not due to the cellular cytotoxicity of dapivirine. Dapivirine was also found to inhibit the B/Brisbane/60/2008 virus with EC<sub>50</sub> value of 1.1 ± 0.1 µM in plaque assay (Fig. 1D). In light of the influenza antiviral activity of dapivirine, we also tested two other closely related HIV NNRTIs, etravirine (Fig. 1B) and rilpivirine (Fig. 1C). Rilpivirine had no antiviral activity against the A/California/07/2009 (H1N1) virus, while etravirine was only active against A/California/07/2009 (H1N1) with an EC<sub>50</sub> value of 6.7 ± 1.7 µM, and it was not active against the B/Brisbane/60/2008 virus (EC<sub>50</sub> > 50 µM) (Fig. 1D). Due to the potent and broad-spectrum antiviral activity of dapivirine, it was selected for following mechanistic studies.

Next, to investigate whether the antiviral activity of dapivirine can be extended to other influenza strains, dapivirine was tested against a panel of thirteen influenza A virus strains and two influenza B virus strains in a plaque assay (Table 1). The viruses chosen include both influenza A and B viruses as well as their subtypes (Table 1) with known drug sensitivity to amantadine and oseltamivir. The list also includes viruses that are resistant to either amantadine or oseltamivir or both. For example, A/Texas/04/2009 (H1N1), A/Washington/29/2009 (H1N1), A/North Carolina/39/2009 (H1N1), and A/Denmark/528/2009 (H1N1) are resistant to both amantadine and oseltamivir, which is conferred by the M2-S31N and NA-H275Y mutations, respectively. The emergence of these multidrug-resistant strains from clinics is of particular concern because they pose a great threat to public health (Hurt, 2014). A/Hong Kong/4801/2014 (H3N2) was also included, and this strain

**Table 1**

EC<sub>50</sub> of dapivirine against a panel of influenza A and B viruses and selection index of dapivirine with MDCK and A549 cell lines.

Influenza Strains	Drug sensitivity	EC <sub>50</sub> (μM) <sup>a</sup>	SI <sup>c</sup>
A/DM/528/2009 (H1N1)	Amantadine	1.3 ± 0.2	11.0
A/Texas/4/2009 (H1N1)	Resistant	1.8 ± 0.3	7.9
A/North Carolina/39/2009 (H1N1)	Oseltamivir	1.1 ± 0.1	13.0
A/Washington/29/2009 (H1N1)	Resistant	1.2 ± 0.2	11.9
A/WSN/1933 (H1N1)	Amantadine	1.8 ± 0.2	7.9
A/California/07/2009 (H1N1)	Resistant	1.2 ± 0.1	11.9
A/DM/524/2009 (H1N1)	Oseltamivir	1.4 ± 0.1	10.2
A/Switzerland/9715293/2013 (H3N2)	Sensitive	1.4 ± 0.2	10.2
A/Switzerland/9715293/2013 X-247 (H3N2)		1.1 ± 0.3	13.0
A/Hongkong/4801/2014 (H3N2)		1.4 ± 0.2 <sup>b</sup>	10.2
A/California/2/2014 (H3N2)		2.2 ± 0.3	6.5
A/Udorn/1972 (H3N2)	Amantadine	1.3 ± 0.4	11.0
A/Soloman Islands/3/2006 (H1N1)	Sensitive	1.5 ± 0.2	9.5
	Oseltamivir		
	Sensitive		
B/Wisconsin/1/2010 (Yamagata)	Amantadine	1.2 ± 0.3	11.9
B/Bris/60/2008 (Victoria)	Resistant	1.1 ± 0.1	13.0
	Oseltamivir		
	Sensitive		

<sup>a</sup> All EC<sub>50</sub> results were determined in plaque assays using the ST6Gal I-overexpressing MDCK cells (AX-4) in 6-well plates; The value is the mean of two independent experiments ± standard deviation.

<sup>b</sup> EC<sub>50</sub> was determined by CPE assay; The value is the mean of two independent experiments ± standard deviation.

<sup>c</sup> SI refers to selectivity index, which is calculated by dividing the 48 h CC<sub>50</sub> of dapivirine using MDCK cells by the EC<sub>50</sub> of dapivirine.

overtakes A/California/07/2009 (H1N1)pdm and becomes the predominant strain in the current 2016–2017 influenza season (<https://www.cdc.gov/flu/weekly/>). The highest drug concentration of dapivirine applied was 3 μM, which confers minimal cellular cytotoxicity (Fig. 3A). Table 1 summarizes the EC<sub>50</sub> values of dapivirine against these viruses as well as the drug sensitivity of these influenza strains toward the approved antiviral drugs amantadine and oseltamivir. Despite their diverse genetic backgrounds and drug sensitivities toward amantadine and oseltamivir, all thirteen influenza A strains and two influenza B strains tested were sensitive to dapivirine with EC<sub>50</sub> values in the range of 1.1–2.2 μM (Table 1). Taken together, these results clearly demonstrate that dapivirine has broad-spectrum antiviral activity against both influenza A and B viruses and has no cross resistance with the currently approved anti-influenza drugs amantadine and oseltamivir. The selectivity index, defined by the ratio of 50% cellular cytotoxicity concentration (CC<sub>50</sub>) over EC<sub>50</sub>, was in the range of 6.5–13.0 (Table 1).

### 3.2. Dapivirine inhibits influenza virus replication in multiple cell lines and with both high and low multiplicity of infection (MOI)

To rule out the possibility that the antiviral activity of dapivirine is cell type-dependent, the antiviral activity of dapivirine was tested in two human cell lines: HEK293 and A549. MDCK cells were included as a reference (Fig. 2). First, the cytotoxicity of dapivirine against these cell lines was determined by the neutral red method (Repetto et al., 2008). The CC<sub>50</sub> values of dapivirine in MDCK cells and human A549 cells were 14.3 ± 0.3 μM and 19.8 ± 2.1 μM, respectively, with a 48 h incubation time (Fig. 2A). Dapivirine was less cytotoxic with a 24 h incubation time, and the CC<sub>50</sub> values of dapivirine in MDCK cells, human HEK293 cells and A549 cells were 27.9 ± 0.7 μM, 25.3 ± 1.4 μM, and 30.8 ± 1.0 μM, respectively (Fig. 2B). Therefore, 3 μM dapivirine, which was the concentration applied for the following antiviral assays in HEK293 and A549 cells, had no effect on cell viability.

When HEK293 cells were infected with the A/California/07/

2009 (H1N1) virus at an MOI of 0.01, 3 μM dapivirine reduced viral titer 2.1 log<sub>10</sub> units at 24 h post infection (p.i.), and the efficacy was comparable to 1 μM oseltamivir carboxylate (Fig. 2C). A similar antiviral effect was observed when A549 cells were infected with the A/WSN/33 (H1N1) virus at an MOI of 0.01 (Fig. 2D), and dapivirine reduced the viral titer by 1.4 log<sub>10</sub> units at 3 μM. When A549 cells were infected with the A/WSN/33 (H1N1) virus at an MOI of 1, dapivirine also showed significant viral inhibition with a reduction of viral titer by 0.7 log<sub>10</sub> unit at 24 h p.i. (Fig. 2D), which was slightly less potent than 1 μM oseltamivir carboxylate. To study the antiviral effect of dapivirine on the kinetics of viral replication, A549 cells were infected with the A/WSN/1933 (H1N1) virus at an MOI of 0.01 (Fig. 2E) and the viral titers were quantified at 12, 24, 48, 72, and 96 h p.i. It was found that 3 μM of dapivirine significantly delayed the viral replication, and the viral titers at 12, 24, and 48 h p.i. were 2.5, 1.4, 0.9 log<sub>10</sub> units lower than the DMSO control, respectively (Fig. 2E). Taken together, these results confirm that dapivirine is capable of inhibiting viral replication in multiple cell lines and with both high and low MOI.

### 3.3. Dapivirine has a high *in vitro* genetic barrier to drug resistance

Antiviral drugs with a high genetic barrier to drug resistance are desired so that they can be used for a longer period of time. To evaluate the *in vitro* genetic barrier to drug resistance of dapivirine, the drug was subjected to serial viral passage experiments with increasing drug selection pressure. Two sets of serial passage experiments were performed (Table 2): one was carried out with the A/WSN/1933 (H1N1) virus, the other was carried out with the A/Switzerland/9715293/2013 (H3N2) virus, which was one of the predominant circulating influenza A strains during the 2014–2015 influenza season in North America. In the passage experiments, the drug concentration of dapivirine was set at 2 μM (equivalent to the EC<sub>50</sub>s) for the first passage and doubled at passages 2 and 3 and was kept constant in passage 4 and onward (Table 2). The reason to set the highest drug concentration at 8 μM was to minimize cellular cytotoxicity (the CC<sub>50</sub> of dapivirine was 14.3 μM for MDCK cells with 48 h incubation time, Fig. 2A). For the passage experiment with the A/WSN/33 (H1N1) virus, the drug sensitivities of resulting viruses at passages 3, 6, 9, and 12 were tested. The EC<sub>50</sub> values of dapivirine against viruses at passages 3, 6, 9, and 12 were 1.55 ± 0.33, 1.28 ± 0.28, 1.69 ± 0.44, and 1.32 ± 0.16 μM, respectively, which were similar to the EC<sub>50</sub> value at passage 0 (1.82 ± 0.20 μM). These results indicate that no resistant viruses were selected. To further confirm this result, another influenza A strain, A/Switzerland/9715293/2013 (H3N2), was passaged in the presence of dapivirine, and oseltamivir carboxylate was included as a control. It was found that the EC<sub>50</sub> values of dapivirine at passages 3 and 6 were similar to that at passage 0. In contrast, a 10-fold increase of EC<sub>50</sub> was observed for oseltamivir carboxylate at passage 6 when similar drug selection pressure was applied, and this result was consistent with previous findings (Ehrhardt et al., 2013; Shih et al., 2010). Collectively, these results indicate dapivirine has a high *in vitro* genetic barrier to drug resistance.

### 3.4. Antiviral mechanism of dapivirine

The broad-spectrum antiviral activity and high *in vitro* genetic barrier to drug resistance of dapivirine render it an interesting drug candidate for further mechanistic studies. To dissect the antiviral mechanism of dapivirine, time-of-addition, immunofluorescence, RT-qPCR, and western blot experiments were performed.

#### 3.4.1. Dapivirine inhibits the early stage of viral replication

To elucidate which stage of the viral replication cycle was

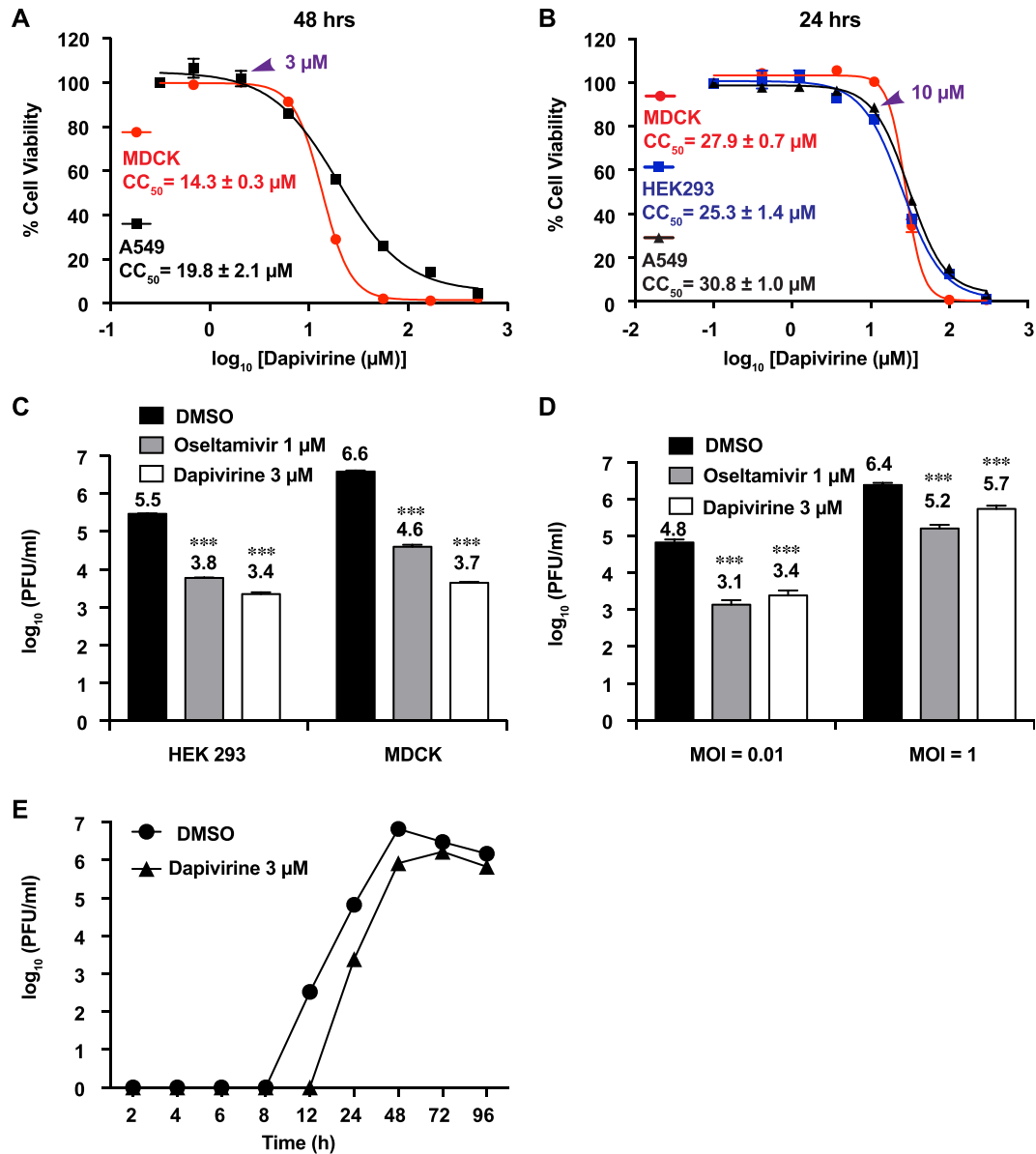


**Fig. 2.** Antiviral activity of dapivirine against A/WSN/1933 (H1N1) and A/California/7/2009 (H1N1) with different cell lines at low and high MOI. (A) CC<sub>50</sub> of dapivirine against MDCK and A549 cell lines with a 48 h incubation time; The CC<sub>50</sub> values are the mean of two independent experiments ± standard deviation. (B) CC<sub>50</sub> of dapivirine against MDCK, HEK293 or A549 cell lines with a 24 h incubation time. The concentration at 3 μM (Figure A) and 10 μM (Figure B) were indicated with arrows. The CC<sub>50</sub> values are the mean of two independent experiments ± standard deviation. (C) HEK293 or MDCK cells were infected with A/California/7/2009 (H1N1) at MOI of 0.01; 3 μM dapivirine or 1 μM oseltamivir carboxylate was added after viral infection. Viruses from supernatant were harvested 24 h p.i. and titers were determined by plaque assay. \*\*\*P < 0.001. The value of viral titer is the mean of two independent experiments ± standard deviation. (D) A549 cells were infected with A/WSN/1933 (H1N1) at MOI of 0.01; 3 μM dapivirine or 1 μM oseltamivir carboxylate was added after viral infection. Viruses from supernatant were harvested 24 h p.i. and the titers were determined by plaque assay. Asterisks indicate statistically significant difference in comparison with the DMSO control (student's t-test, \*\*\*P < 0.001). The value of viral titer is the mean of two independent experiments ± standard deviation. (E) A549 cells were infected with A/WSN/1933 (H1N1) at MOI of 0.01; DMSO (control) or 3 μM dapivirine was added after infection. Viruses from supernatant were harvested 2, 4, 6, 8, 12, 24, 48, 72, or 96 h post infection. Virus titers were determined by plaque assay.

inhibited by dapivirine, a time-of-addition experiment was performed. In this experiment, dapivirine was added either before viral replication or at different time points during and after viral infection. Specifically, MDCK cells were infected with the A/WSN/1933 (H1N1) virus at MOI of 0.01 at -2 h time point, and viruses were harvested at 12 h p.i. and the viral titer was quantified by plaque assay. Oseltamivir carboxylate was included as a control. Consistent with its mechanism of inhibiting the late stage of viral replication by preventing the release of progeny virion (Sidwell et al., 1998), oseltamivir carboxylate retained potent antiviral activity even when it was added 8 h post viral infection (Fig. 3A). In contrast, the

antiviral efficacy of dapivirine gradually decreased when it was added at later stages of viral replication (Fig. 3B). Nevertheless, even when added 8 h p.i., dapivirine remained effective in suppressing viral replication, and a 1.5 log<sub>10</sub> unit viral titer reduction was observed. Dapivirine had no effect on viral attachment, and entry as drug treatment during -2 to 0 h had no effect on viral titer (Fig. 3B). In addition, pretreatment of MDCK cells from either -24 to -2 h or -12 to -2 h had no effect on viral replication. Overall, the time-of-addition experiments suggest that dapivirine inhibits the early stage of influenza virus replication post viral entry, possibly by interfering with the viral RNA replication and transcription.

**Table 2**  
Serial viral passage experiments with dapivirine drug selection pressure.

Set 1: A/WSN/1933 (H1N1)			Set 2: A/Switzerland/9715293/2013 (H3N2)				
Passage number	dapivirine (μM)	EC <sub>50</sub> (μM) <sup>a</sup>	Passage number	dapivirine (μM)	EC <sub>50</sub> (μM) <sup>a</sup>	Osetamivir (nM)	EC <sub>50</sub> (nM) <sup>a</sup>
0	0	1.82 ± 0.20	0	0	1.42 ± 0.20	0	12 ± 5
1	2	N.D.	1	2	N.D.	15	N.D.
2	4	N.D.	2	4	N.D.	30	N.D.
3	8	1.55 ± 0.33	3	8	1.40 ± 0.14	60	175 ± 53
4	8	N.D.	4	8	N.D.	120	N.D.
5	8	N.D.	5	8	N.D.	120	N.D.
6	8	1.28 ± 0.28	6	8	1.73 ± 0.10	120	260 ± 77
7	8	N.D.					
8	8	N.D.					
9	8	1.69 ± 0.44					
10	8	N.D.					
11	8	N.D.					
12	8	1.32 ± 0.16					

<sup>a</sup> The EC<sub>50</sub> value is the mean of two independent experiments ± standard deviation.

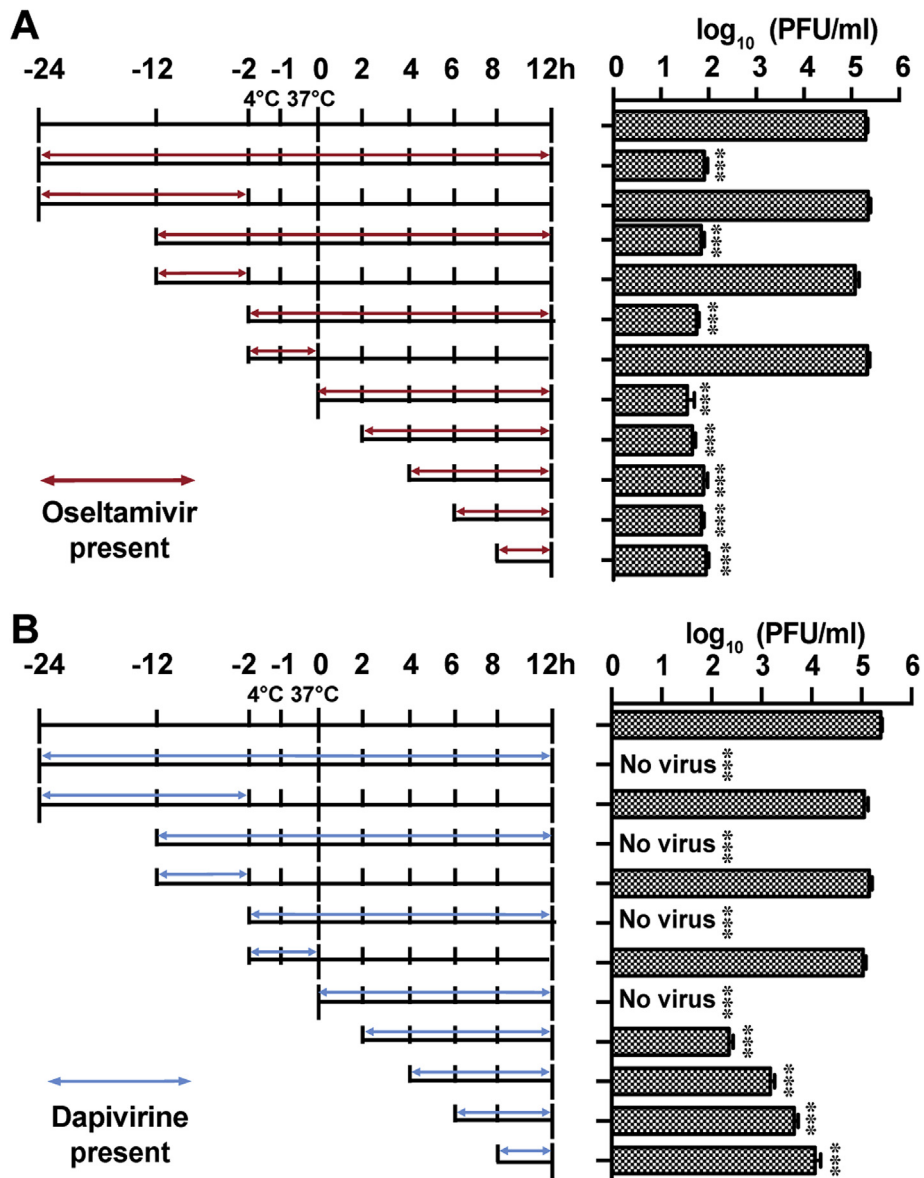


**Fig. 3. Time-of-addition experiments.** MDCK cells were infected with the A/WSN/33 (H1N1) virus at –2 h time point; viruses were first incubated at 4 °C for 1 h for attachment followed by 37 °C for 1 h for viral entry. At time point 0 h, cells were washed with PBS buffer and viruses were harvested at 12 h p.i. The titer of harvested virus was determined by plaque assay. Arrows indicate the period in which (A) 1 μM oseltamivir carboxylate or (B) 3 μM dapivirine was present. Asterisks indicate statistically significant difference in comparison with the DMSO control (student's t-test, \*\*\*P < 0.001). The value of viral titer is the mean of two independent experiments ± standard deviation.

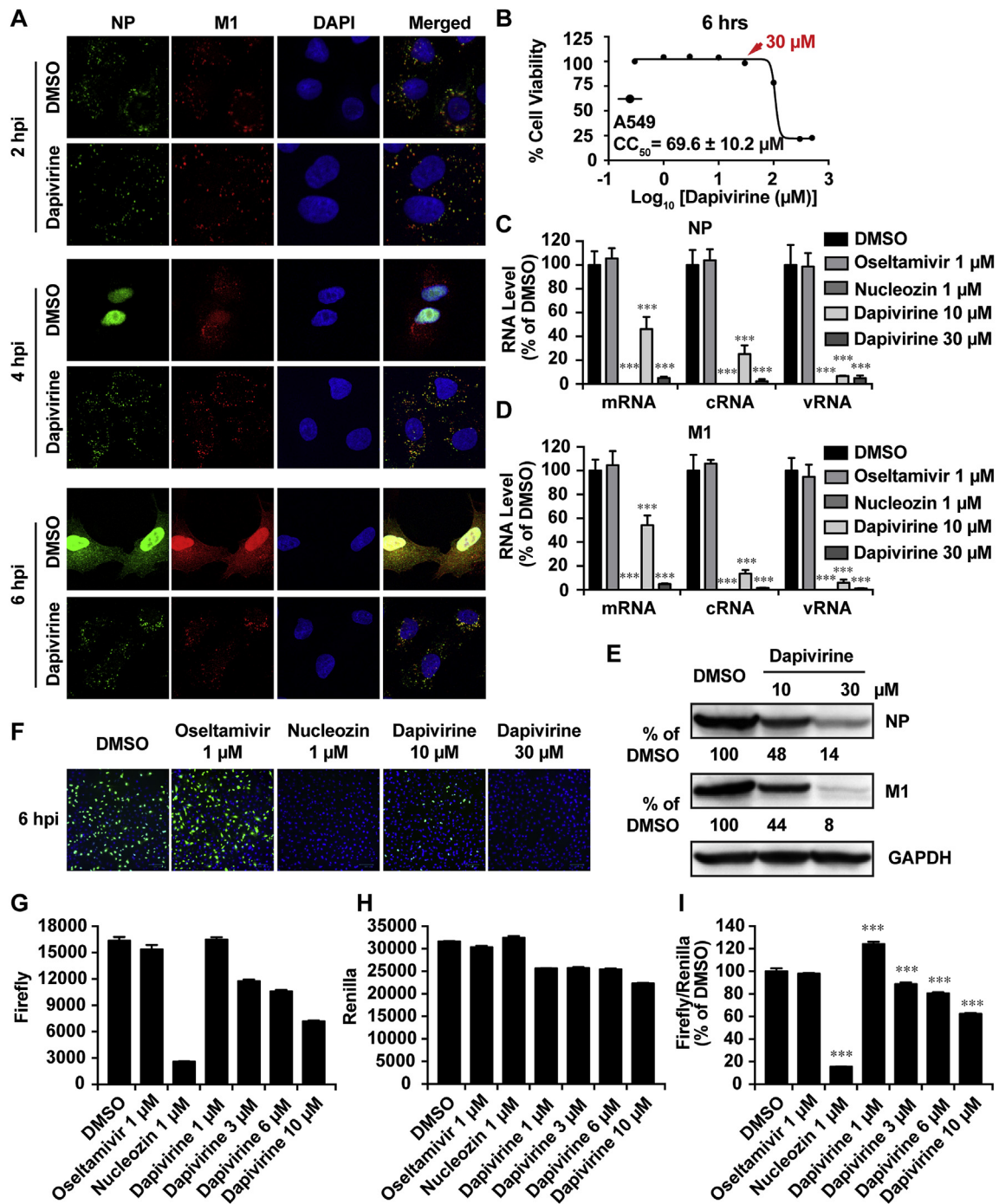


**Fig. 4. Dapivirine inhibited the nuclear entry of vRNP complex at the early stage of viral replication.** (A) Retention of influenza vRNPs in cytoplasm by dapivirine. A549 cells infected with the A/WSN/33 (H1N1) virus (MOI = 30) were treated with DMSO or 30 µM of dapivirine. After fixation at indicated times (2, 4, and 6 h p.i.), cells were stained with mouse anti-influenza A NP antibody, rabbit anti-M1, and DAPI to determine the viral NP, M1 protein, and nucleus, respectively. (B) CC<sub>50</sub> of dapivirine against A549 cell line with a 6 h incubation time. The concentration at 30 µM was indicated with an arrow. The CC<sub>50</sub> value is the mean of two independent experiments ± standard deviation. (C–F) Dapivirine reduced the levels of viral RNAs and proteins. A549 cells infected with the A/WSN/33 (H1N1) virus (MOI = 1) were treated with DMSO and 10 or 30 µM of dapivirine. At 6 h p.i., cells were harvested and total viral RNA was extracted and quantified by RT-qPCR (C and D). Asterisks indicate statistically significant difference in comparison with the DMSO control (student's t-test, \*\*\*P < 0.001). The value of RNA level is the mean of two independent experiments ± standard deviation. Viral protein levels were quantified by western blot (E) and immunofluorescence (F). (G–I) Mini-genome assay. A549 cells were transfected with a combination of plasmids for minigenome assay (see in Materials and Methods). Dapivirine was added to the culture medium at 2 h post transfection. After 22 h incubation, cells were harvest and the activities of Firefly (G) and Renilla (H) luciferases were measured using the dual luciferase kit from Promega. Renilla was served as an internal control to normalize the transfection efficiency (I). Asterisks indicate statistically significant difference in comparison with the DMSO control (student's t-test, \*\*\*P < 0.001). The value of luciferase signal is the mean of two independent experiments ± standard deviation.

**Table 3**  
Antiviral results of combinational treatments.

Combination Ratio (EC <sub>50</sub> )	EC <sub>50</sub> in Combination		EC <sub>50</sub> alone		EC <sub>50</sub> Equivalent <sup>a</sup>		FICI <sup>b</sup>	
	Osetamivir: Dapivirine	Dapivirine (μM)	Osetamivir (nM)	Dapivirine (μM)	Osetamivir (nM)	Dapivirine		Osetamivir
10:1		0.018 ± 0.003	1.57 ± 0.2	5.9 ± 0.2	4.4 ± 0.5	0.003	0.357	0.36
5:1		0.036 ± 0.009	1.78 ± 0.4			0.006	0.405	0.41
1:1		0.47 ± 0.3	0.8 ± 0.2			0.080	0.182	0.26
1:5		0.66 ± 0.05	1.31 ± 0.1			0.112	0.298	0.41
1:10		1.19 ± 0.2	1.19 ± 0.2			0.202	0.270	0.47

Values are means of two independent experiments ± standard deviation.

<sup>a</sup> Concentration in EC<sub>50</sub> equivalent was the normalized concentration that was calculated by dividing the EC<sub>50</sub> of drug in combination with its EC<sub>50</sub> alone.

<sup>b</sup> FICI was the sum of dapivirine and oseltamivir EC<sub>50</sub> equivalent concentrations used in each combination.

### 3.4.2. Dapivirine inhibits viral RNA transcription and viral protein synthesis

To determine whether dapivirine interferes with the nuclear localization of the vRNP complex at different stages of viral replication, an immunofluorescence imaging assay was carried out (Fig. 4A). In this experiment, A549 cells were infected with the A/WSN/33 (H1N1) virus with an MOI of 30. Dapivirine was tested at 30 μM, which had no effect on cell viability within the 6 h drug treatment experiment (Fig. 4B). The cells were fixed at 2, 4, and 6 h p.i., and the viral proteins NP and M1 were stained with anti-NP and anti-M1 antibodies, respectively. It was found that dapivirine inhibits the nuclear entry of vRNP at 4 h p.i. and the NP protein remained in the cytoplasm with the dapivirine-treated sample (Fig. 4A), while in the DMSO control sample, a clear nuclear localization of NP protein was observed. At 6 h p.i., the newly synthesized vRNP started to exit the nucleus in the DMSO control sample, while in the dapivirine-treated sample, NP remained in the cytoplasm. Likewise, dapivirine also inhibited the M1 localization at 2, 4, and 6 h p.i. Previous studies have shown that M1 is not required for the early stage of viral RNA transcription and translation, but it is transported to the nucleus to help with the exit of newly synthesized vRNP complex at the later stage of viral replication (Eisfeld et al., 2015). A clear nuclear localization of M1 protein in the DMSO control sample was observed at 4 h p.i. (Fig. 4A), while in the dapivirine-treated sample M1 protein remained predominantly in the cytoplasm. At 6 h p.i., the newly synthesized M1 protein was found in both the nucleus and the cytoplasm in the DMSO control sample. In contrast, the M1 immunofluorescence signal was much lower in the dapivirine-treated sample and the M1 protein remained in the cytoplasm. The immunofluorescence assay results of dapivirine suggest that it inhibits the nuclear entry of vRNP at the early stage of viral replication and it also inhibits viral protein synthesis. To further confirm this observation, RT-qPCR and western blot experiments were conducted to quantify viral RNA and protein levels with and without dapivirine treatment. If dapivirine indeed inhibits the nuclear entry of vRNP, viral RNA and protein levels should be reduced. Indeed, dapivirine inhibited both NP and M1 RNA levels in a dose-dependent manner, as shown by RT-qPCR (Fig. 4C and D). As a result, both the NP and M1 protein levels were reduced (Fig. 4E). The inhibition of NP protein synthesis was further confirmed by immunofluorescence assay (Fig. 4F). The inhibition of NP protein synthesis was dose dependent, and nearly complete inhibition was observed at 30 μM dapivirine. Nucleozin, a known inhibitor of NP protein, was included as a positive control and completely inhibited viral NP protein synthesis at 1 μM. Collectively, these results indicate that dapivirine inhibits the early stage of viral replication by preventing the nuclear entry of the vRNP complex, thereby inhibiting both viral RNA and protein synthesis. To further investigate whether dapivirine directly inhibits influenza

polymerase activity, the mini-genome assay was conducted.

### 3.4.3. Dapivirine inhibits viral polymerase activity in the mini-genome assay

The mini-genome assay (also called mini-replicon assay) is a standard assay to quantify viral polymerase activity and to test whether a compound inhibits viral polymerase activity (Beyleveld et al., 2013; Hoffmann et al., 2011). In the mini-genome assay, HEK 293 T cells were transfected with six plasmids, four of which encode the viral polymerase complex NP, PA, PB1, and PB2, one plasmid encoding the influenza virus-specific RNA polymerase I-driven firefly luciferase reporter (vRNA Luc), and one plasmid encoding the RNA polymerase II-driven Renilla luciferase reporter pRL-SV40, which was used to normalize the transfection efficiency. Nucleozin, which has been shown to inhibit viral polymerase activity in the mini-genome assay (Kao et al., 2010), was included as a positive control. As shown in Fig. 4G–I, nucleozin nearly completely inhibits the viral polymerase activity at 1 μM. Dapivirine also showed dose-dependent inhibition with a 40% reduction of polymerase activity at 10 μM drug concentration. A further increase of the dapivirine concentration to 20 μM led to cellular cytotoxicity (Fig. 2B). It was noted that a 20% reduction of renilla luciferase activity was observed when the cells were treated with 10 μM dapivirine, which suggests dapivirine might inhibit host protein synthesis at high drug concentrations. In summary, the mini-genome assay results are consistent with the immunofluorescence, RT-qPCR, and western blot assay results, which suggests that dapivirine inhibits viral polymerase activity by preventing the nuclear entry of the vRNP complex.

### 3.5. Dapivirine has synergistic antiviral effect with oseltamivir carboxylate in vitro

As the antiviral mechanism of dapivirine is distinct from that of oseltamivir, we were interested in exploring whether the antiviral effect of dapivirine is synergistic, additive, or antagonistic with oseltamivir. For this purpose, we investigated the *in vitro* combination therapy potential of dapivirine and oseltamivir carboxylate by calculating the fractional inhibitory concentration index (FICI) (Huggins et al., 1984) (Meletiadis et al., 2010) (Table 3). FICI is one of the standard methodologies in evaluating the drug–drug combination, and it provides quantitative estimation of the extent of synergy or antagonism (Fouquier and Guedj, 2015; Zhao et al., 2010). Loewe additive zero-interaction theory is the basis for the FICI method and is used to analyze drug–drug interaction. FICI less than, equal to, or greater than 1 indicates synergy, additivity, or antagonism, respectively (Berenbaum, 1989). In this study, five sets of combinations of dapivirine and oseltamivir carboxylate were conducted, and FICI of each set was determined. As shown in Table 3, all tested combinations resulted in FICI that <0.5, indicating strong synergism between dapivirine and oseltamivir carboxylate.

#### 4. Discussion and conclusion

Despite the availability of influenza vaccines and small-molecule antiviral drugs, each year an estimated 5–10% of adults and 20–30% of children are infected with influenza viruses, which results in 250–500 thousand deaths (<http://www.who.int/mediacentre/factsheets/fs211/en/>). Therefore, effective antiviral drugs with a novel mechanism of action are clearly needed to combat both existing and potential drug-resistant influenza viruses. To offset the cost and time of drug discovery, drug repurposing that applies known drugs for the treatment of new diseases is one such fast-track strategy (Ashburn and Thor, 2004) (Shim and Liu, 2014). Here, we discovered dapivirine, an HIV NNRTI, as a broad-spectrum influenza antiviral with a high *in vitro* genetic barrier to drug resistance.

In our work, the broad-spectrum antiviral activity and high *in vitro* genetic barrier to drug resistance of dapivirine appear to suggest that dapivirine is a host-targeting antiviral, although we cannot completely rule out the possibility that dapivirine also targets viral proteins. Mechanistic studies show that dapivirine inhibits the early stage of viral replication post viral entry. Specifically, dapivirine treatment led to the inhibition of nuclear entry of the vRNP complex at the early stage of viral replication, as shown by an immunofluorescence assay. As a result, viral RNA replication and transcription, as well as viral protein synthesis, were inhibited. These results were consistent with the time-of-addition experiment, which showed that the antiviral effect of dapivirine gradually decreased when it was added at the later stages of viral replication. The proposed antiviral mechanism of dapivirine was further corroborated by the mini-genome assay results. Encouragingly, the antiviral effect of dapivirine was synergistic with oseltamivir carboxylate, suggesting that dapivirine can be used either alone to treat infections with oseltamivir-resistant strains or in combination with oseltamivir to delay drug resistance in oseltamivir-sensitive strains.

Due to its poor oral bioavailability, dapivirine is being developed as a topical agent. Relevant to the treatment of influenza virus infection, it is desired to optimize dapivirine as an orally bioavailable drug, which could be achieved by structure–activity–relationship studies.

It is important to highlight that a dual HIV- and influenza-acting drug such as dapivirine offers additional therapeutic benefits for HIV patients. Although HIV infection does not significantly increase the susceptibility of subsequent influenza virus infection, influenza virus infection in HIV patients does lead to increased mortality and mobility rates (Kunisaki and Janoff, 2009; Sheth et al., 2011; Trebbien et al., 2017). This is largely due to the compromised immune system of HIV patients, which renders them incapable of suppressing viral replication. For this reason, extended treatment with influenza antivirals is required. However, prolonged administration of direct-acting influenza antivirals such as oseltamivir and zanamivir has been shown to lead to the emergence of drug resistance (Trebbien et al., 2017). Therefore, a dual HIV and influenza drug that could not only suppress HIV but also inhibit influenza virus replication is highly desired. The discovery of dapivirine as a broad-spectrum influenza antiviral offers an opportunity to develop such dual-targeting drugs, and further development of dapivirine analogs is warranted.

#### Acknowledgements

This work was supported by University of Arizona startup funds and NIH AI 119187 to J.W. R.M. was supported by the NIH training grant T32 GM008804. We thank David Bishop for proofreading and editing the manuscript.

#### References

- Ashburn, T.T., Thor, K.B., 2004. Drug repositioning: identifying and developing new uses for existing drugs. *Nat. Rev. Drug. Discov.* 3, 673–683.
- Baeten, J.M., Palanee-Phillips, T., Brown, E.R., Schwartz, K., Soto-Torres, L.E., Govender, V., Mgodini, N.M., Matovu Kiweewa, F., Nair, G., Mhlanga, F., Siva, S., Bekker, L.G., Jeenaarain, N., Gaffoor, Z., Martinson, F., Makanani, B., Pather, A., Naidoo, L., Husnik, M., Richardson, B.A., Parikh, U.M., Mellors, J.W., Marzinke, M.A., Hendrix, C.W., van der Straten, A., Ramjee, G., Chirenje, Z.M., Nakabiito, C., Taha, T.E., Jones, J., Mayo, A., Sheckter, R., Berthiaume, J., Livant, E., Jacobson, C., Ndase, P., White, R., Patterson, K., Germuga, D., Galaska, B., Bunge, K., Singh, D., Szydlo, D.W., Montgomery, E.T., Mensch, B.S., Torjesen, K., Grossman, C.I., Chakhtoura, N., Nel, A., Rosenberg, Z., McGowan, I., Hillier, S., Team, M.-A.S., 2016. Use of a vaginal ring containing dapivirine for HIV-1 prevention in women. *N. Engl. J. Med.* 375, 2121–2132.
- Berenbaum, M.C., 1989. What is synergy? *Pharmacol. Rev.* 41, 93–141.
- Beyleveld, G., White, K.M., Ayllon, J., Shaw, M.L., 2013. New-generation screening assays for the detection of anti-influenza compounds targeting viral and host functions. *Antivir. Res.* 100, 120–132.
- Bloom, J.D., Gong, L.L., Baltimore, D., 2010. Permissive secondary mutations enable the evolution of influenza oseltamivir resistance. *Science* 328, 1272–1275.
- D'Andrea, G., Brisdeli, F., Bozzi, A., 2008. AZT: an old drug with new perspectives. *Curr. Clin. Pharmacol.* 3, 20–37.
- Dawood, F.S., Iuliano, A.D., Reed, C., Meltzer, M.I., Shay, D.K., Cheng, P.Y., Bandaranayake, D., Breiman, R.F., Brooks, W.A., Buchy, P., Feikin, D.R., Fowler, K.B., Gordon, A., Hien, N.T., Horby, P., Huang, Q.S., Katz, M.A., Krishnan, A., Lal, R., Montgomery, J.M., Molbak, K., Pebody, R., Presanis, A.M., Razuri, H., Steens, A., Tinoco, Y.O., Wallinga, J., Yu, H., Vong, S., Bresee, J., Widdowson, M.A., 2012. Estimated global mortality associated with the first 12 months of 2009 pandemic influenza A H1N1 virus circulation: a modelling study. *Lancet Infect. Dis.* 12, 687–695.
- Ehrhardt, C., Ruckle, A., Hrcincus, E.R., Haasbach, E., Anhlan, D., Ahmann, K., Banning, C., Reiling, S.J., Kuhn, J., Strobl, S., Vitt, D., Leban, J., Planz, O., Ludwig, S., 2013. The NF-kappaB inhibitor SC75741 efficiently blocks influenza virus propagation and confers a high barrier for development of viral resistance. *Cell. Microbiol.* 15, 1198–1211.
- Eisfeld, A.J., Neumann, G., Kawaoka, Y., 2015. At the centre: influenza A virus ribonucleoproteins. *Nat. Rev. Microbiol.* 13, 28–41.
- Fink, H.A., Mac Donald, R., Rutks, I.R., Nelson, D.B., Wilt, T.J., 2002. Sildenafil for male erectile dysfunction: a systematic review and meta-analysis. *Arch. Intern. Med.* 162, 1349–1360.
- Fouquier, J., Guedj, M., 2015. Analysis of drug combinations: current methodological landscape. *Pharmacol. Res. Perspect.* 3, e00149.
- Grohskopf, L.A., Sokolow, L.Z., Olsen, S.J., Bresee, J.S., Broder, K.R., Karron, R.A., 2015. Prevention and control of influenza with vaccines: recommendations of the advisory committee on immunization practices, United States, 2015–16 influenza season. *MMWR Morb. Mortal. Wkly. Rep.* 64, 818–825.
- Hay, A.J., Hayden, F.G., 2013. Oseltamivir resistance during treatment of H7N9 infection. *Lancet* 381, 2230–2232.
- Hoffmann, H.H., Kunz, A., Simon, V.A., Palese, P., Shaw, M.L., 2011. Broad-spectrum antiviral that interferes with de novo pyrimidine biosynthesis. *Proc. Natl. Acad. Sci. U. S. A.* 108, 5777–5782.
- <http://www.who.int/mediacentre/factsheets/fs211/en/>.
- Hu, Y., Musharrafieh, R., Ma, C., Zhang, J., Smeek, D.F., DeGrado, W.F., Wang, J., 2017. An M2-V27A channel blocker demonstrates potent *in vitro* and *in vivo* antiviral activities against amantadine-sensitive and -resistant influenza A viruses. *Antivir. Res.* 140, 45–54.
- Huggins, J.W., Robins, R.K., Canonico, P.G., 1984. Synergistic antiviral effects of ribavirin and the C-nucleoside analogs tiazofurin and selenazofurin against togaviruses, bunyaviruses, and arenaviruses. *Antimicrob. Agents Chemother.* 26, 476–480.
- Hurt, A.C., 2014. The epidemiology and spread of drug resistant human influenza viruses. *Curr. Opin. Virol.* 8, 22–29.
- Johnson, N.P., Mueller, J., 2002. Updating the accounts: global mortality of the 1918–1920 “Spanish” influenza pandemic. *Bull. Hist. Med.* 76, 105–115.
- Kao, R.Y., Yang, D., Lau, L.S., Tsui, W.H., Hu, L., Dai, J., Chan, M.P., Chan, C.M., Wang, P., Zheng, B.J., Sun, J., Huang, J.D., Madar, J., Chen, G., Chen, H., Guan, Y., Yuen, K.Y., 2010. Identification of influenza A nucleoprotein as an antiviral target. *Nat. Biotechnol.* 28, 600–605.
- Koutsakos, M., Nguyen, T.H., Barclay, W.S., Kedzierska, K., 2016. Knowns and unknowns of influenza B viruses. *Future Microbiol.* 11, 119–135.
- Kunisaki, K.M., Janoff, E.N., 2009. Influenza in immunosuppressed populations: a review of infection frequency, morbidity, mortality, and vaccine responses. *Lancet Infect. Dis.* 9, 493–504.
- Lambert, L., Fauci, A., 2010. Current concepts influenza vaccines for the future. *N. Engl. J. Med.* 363, 2036–2044.
- Lauring, A.S., Andino, R., 2010. Quasispecies theory and the behavior of RNA viruses. *PLoS Pathog.* 6, e1001005.
- Li, F., Hu, Y., Wang, Y., Ma, C., Wang, J., 2017. Expedient lead optimization of isoxazole-containing influenza A virus M2-S31N inhibitors using the Suzuki-Miyaura cross-coupling reaction. *J. Med. Chem.* 60, 1580–1590.
- Li, F., Ma, C., DeGrado, W.F., Wang, J., 2016. Discovery of highly potent inhibitors targeting the predominant drug-resistant S31N mutant of the influenza A virus M2 proton channel. *J. Med. Chem.* 59, 1207–1216.

- Loregian, A., Mercorelli, B., Nannetti, G., Compagnin, C., Palu, G., 2014. Antiviral strategies against influenza virus: towards new therapeutic approaches. *Cell. Mol. Life Sci.* 71, 3659–3683.
- Ma, C., Li, F., Musharrafieh, R.G., Wang, J., 2016a. Discovery of cyclosporine A and its analogs as broad-spectrum anti-influenza drugs with a high in vitro genetic barrier of drug resistance. *Antivir. Res.* 133, 62–72.
- Ma, C., Zhang, J., Wang, J., 2016b. Pharmacological characterization of the spectrum of antiviral activity and genetic barrier to drug resistance of M2-S31N channel blockers. *Mol. Pharmacol.* 90, 188–198.
- Matsuzaki, Y., Katsushima, N., Nagai, Y., Shoji, M., Itagaki, T., Sakamoto, M., Kitaoka, S., Mizuta, K., Nishimura, H., 2006. Clinical features of influenza C virus infection in children. *J. Infect. Dis.* 193, 1229–1235.
- Meletiadiis, J., Pournaras, S., Roilides, E., Walsh, T.J., 2010. Defining fractional inhibitory concentration index cutoffs for additive interactions based on self-drug additive combinations, Monte Carlo simulation analysis, and in vitro in vivo correlation data for antifungal drug combinations against *Aspergillus fumigatus*. *Antimicrob. Agents Chemother.* 54, 602–609.
- Nel, A., van Niekerk, N., Kapiga, S., Bekker, L.G., Gama, C., Gill, K., Kamali, A., Kotze, P., Louw, C., Mabude, Z., Miti, N., Kusemererwa, S., Tempelman, H., Carstens, H., Devlin, B., Isaacs, M., Malherbe, M., Mans, W., Nuttall, J., Russell, M., Ntshelhe, S., Smit, M., Solai, L., Spence, P., Steytler, J., Windle, K., Borremans, M., Resselers, S., Van Roey, J., Parys, W., Vangeneugden, T., Van Baelen, B., Rosenberg, Z., Ring Study, T., 2016. Safety and efficacy of a dapivirine vaginal ring for HIV prevention in women. *N. Engl. J. Med.* 375, 2133–2143.
- Novac, N., 2013. Challenges and opportunities of drug repositioning. *Trends Pharmacol. Sci.* 34, 267–272.
- Odds, F.C., 2003. Synergy, antagonism, and what the checkerboard puts between them. *J. Antimicrob. Chemother.* 52, 1.
- Ormsby, C.E., de la Rosa-Zamboni, D., Vazquez-Perez, J., Ablanedo-Terrazas, Y., Vega-Barrientos, R., Gomez-Palacio, M., Murakami-Ogasawara, A., Ibarra-Avalos, J.A., Romero-Rodriguez, D., Avila-Rios, S., Reyes-Teran, G., 2011. Severe 2009 pandemic influenza A (H1N1) infection and increased mortality in patients with late and advanced HIV disease. *AIDS* 25, 435–439.
- Osterholm, M., Kelley, N., Sommer, A., Belongia, E., 2012. Efficacy and effectiveness of influenza vaccines: a systematic review and meta-analysis. *Lancet Infect. Dis.* 12, 36–44.
- Palese, P., Shaw, M.L., 2007. Orthomyxoviridae: the viruses and their replication. In: Knipe, D.M., Howley, P.M. (Eds.), *Fields Virology*, fifth ed. Lippincott Williams & Wilkins, Philadelphia, pp. 1647–1690.
- Repetto, G., del Peso, A., Zurita, J.L., 2008. Neutral red uptake assay for the estimation of cell viability/cytotoxicity. *Nat. Protoc.* 3, 1125–1131.
- Samson, M., Pizzorno, A., Abed, Y., Boivin, G., 2013. Influenza virus resistance to neuraminidase inhibitors. *Antivir. Res.* 98, 174–185.
- Sheth, A.N., Althoff, K.N., Brooks, J.T., 2011. Influenza susceptibility, severity, and shedding in HIV-infected adults: a review of the literature. *Clin. Infect. Dis.* 52, 219–227.
- Shih, S.R., Horng, J.T., Poon, L.L., Chen, T.C., Yeh, J.Y., Hsieh, H.P., Tseng, S.N., Chiang, C., Li, W.L., Chao, Y.S., Hsu, J.T., 2010. BPR2-D2 targeting viral ribonucleoprotein complex-associated function inhibits oseltamivir-resistant influenza viruses. *J. Antimicrob. Chemother.* 65, 63–71.
- Shim, J.S., Liu, J.O., 2014. Recent advances in drug repositioning for the discovery of new anticancer drugs. *Int. J. Biol. Sci.* 10, 654–663.
- Shuji Hatakeyama, Y.S.-T., Kiso, Maki, Goto, Hideo, Kawakami, Chiharu, Mitamura, Keiko, Sugaya, Norio, Suzuki, Yasuo, Kawaoka, Yoshihiro, 2015. Enhanced expression of an  $\alpha$ 2,6-linked sialic acid on MDCK cells improves isolation of human influenza viruses and evaluation of their sensitivity to a neuraminidase inhibitor. *J. Clin. Microbiol.* 43 (8), 4139–4146.
- Sidwell, R.W., Huffman, J.H., Barnard, D.L., Bailey, K.W., Wong, M.H., Morrison, A., Syndergaard, T., Kim, C.U., 1998. Inhibition of influenza virus infections in mice by GS4104, an orally effective influenza virus neuraminidase inhibitor. *Antivir. Res.* 37, 107–120.
- Thompson, M.G., Shay, D.K., Zhou, H., Bridges, C.B., Cheng, P.Y., Burns, E., Bresee, J.S., Cox, N.J., 2010. Estimates of deaths associated with seasonal influenza—United States, 1976–2007 (reprinted from *MMWR*, vol. 59, pg 1057–1062, 2010). *JAMA* 304, 1778–1780.
- Trebbien, R., Pedersen, S.S., Vorborg, K., Franck, K.T., Fischer, T.K., 2017. Development of oseltamivir and zanamivir resistance in influenza A(H1N1)pdm09 virus, Denmark, 2014. *Euro Surveill.* 22, 30445.
- van Kampen, J.J., Bielefeld-Buss, A.J., Ott, A., Maaskant, J., Faber, H.J., Lutsan, J.G., Boucher, C.A., 2013. Case report: oseltamivir-induced resistant pandemic influenza A (H1N1) virus infection in a patient with AIDS and *Pneumocystis jirovecii* pneumonia. *J. Med. Virol.* 85, 941–943.
- Wang, J., Li, F., Ma, C., 2015. Recent progress in designing inhibitors that target the drug-resistant M2 proton channels from the influenza A viruses. *Biopolymers* 104, 291–309.
- Wang, J., Qiu, J.X., Soto, C., DeGrado, W.F., 2011. Structural and dynamic mechanisms for the function and inhibition of the M2 proton channel from influenza A virus. *Curr. Opin. Struct. Biol.* 21, 68–80.
- Wong, S., Webby, R., 2013. Traditional and new influenza vaccines. *Clin. Microbiol. Rev.* 26, 476–492.
- Zhao, L., Au, J.L., Wientjes, M.G., 2010. Comparison of methods for evaluating drug-drug interaction. *Front. Biosci. (Elite Ed.)* 2, 241–249.